

# Applied Mathematics & Information Sciences An International Journal

http://dx.doi.org/10.18576/amis/190614

# Effects of Generation/Absorption on a MHD Flow and Heat Transfer for a Convective Powell-Eyring Fluid with Variable Properties over a Stretching Sheet with a Slip Velocity

Abeer S. Elfeshawey and Shimaa E. Waheed\*

Department of Mathematics, Faculty of Science, Benha University, Benha(13518), Egypt

Received: 2 Jul. 2021, Revised: 2 Sep. 2021, Accepted: 27 Oct. 2021

Published online: 1 Nov. 2025

**Abstract:** The influences of temperature dependent viscosity and thermal conductivity on a steady magnetohydrodynamic (MHD) flow of a non-Newtonian Powell-Eyring fluid with heat transfer, and slip velocity over a stretching sheet located in a porous medium is studied. Certain transformations are employed to transform the governing partial differential equations to an ordinary form. The numerical solutions for the ordinary differential equations are obtained using shooting method with fourth order RungeKutta scheme, and compared with some of analytical solutions. The numerical results are then discussed graphically in the form of velocity and temperature fields for several physical parameters of interest, and numerical data for the local skin-friction coefficient and the local Nusselt number have been tabulated for various values of parametric conditions.

Keywords: Non Newtonian Powell-Eyring fluid; Variable properties; Heat generation/absorption; Slip velocity.

### 1 Introduction

Recently, the study of fluid flow and heat transfer past a stretching sheet has been focused by a large amount of researches due to its significance in many industrial and engineering applications. Some of such numerous practical applications may be observed in hot rolling, drawing of plastic films, annealing and tinning of copper wires, metal spinning and paper production [1]. So, A large number of papers concerned with the fluid flow and heat transfer over a stretching sheet. These have been reported in the previous literatures [2]-[5].

Due to the importance of non-Newtonian fluid flow in numerous engineering and industrial applications, this type of fluids has prominent studies in recent years. One of these fluids is a Powell-Eyring fluid, in this type the mathematical model describing the flow behaviour at low and high shear rates is very complex in its nature. Powell and Eyring [6] were the first researchers postulate the foundation of this type of fluid. Additionally, they reported that this type of fluid can be used to describe the flows of modern industrial materials such as ethylene

glycol and powdered graphite. During the past years, numerous studies related to investigators have already applied some of physical assumptions in this type of fluid [7]-[13], the most recent studies in this fluid for various surfaces being that [14]-[17].

The purpose of the present paper is to study a problem includes the simultaneous effects generation/absorption and slip velocity non-Newtonian Powell-Eyring fluid. The problem under consideration is that of fully developed Powell-Eyring fluid flow and heat transfer over a stretching sheet which is heated by means of a convection boundary condition and the model is imbedded in a porous medium. Effect of magnetic field is assumed in the analysis; thus, it might justifiably be argued that such an assumption is highly restrictive. However, it is felt that a non-Newtonian thermal convection study which includes the effects of slip velocity even for variable properties is of considerable interest.

<sup>\*</sup> Corresponding author e-mail: shimaa\_ezat@yahoo.com



# 2 Mathematical Analysis

Consider the study two dimensional flow of an incompressible MHD Powell-Eyring fluid in porous space, this study will be in the boundary layer between a free stream and horizontal stretching sheet of velocity  $u_w = ax$  (a is a stretching constant). The plate coincide with the plane y > 0 in the presence of heat source and a uniform magnetic field B is applied normal to the plate, the magnetic Reynolds number of the flow is taken to be small enough so that the induced magnetic field is assumed to be negligible. The x -axis is taken along the direction of motion, the y -axis is taken normal to the surface, u, v denote the respective velocity. The down surface of the plate is heated by convection from a hot fluid of temperature  $T_f$  giving a heat transfer coefficient  $h_f$ , as shown in Fig.1.

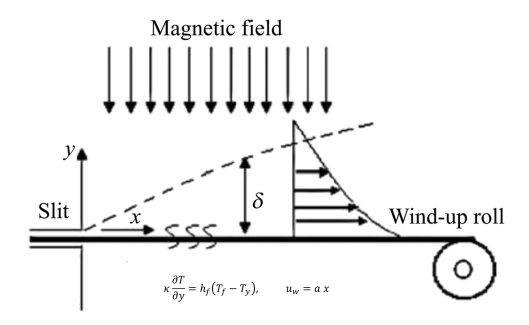


Fig. 1: Flow configuration and coordinate system

In the Powell-Eyring model, the fluid stress tensor  $\tau_{xy}$ can be written as

$$\tau_{xy} = \mu \frac{\partial u}{\partial y} + \frac{1}{\widetilde{\beta}c} Sinh^{-1} \frac{\partial u}{\partial y}$$
 (1)

where  $\mu$  is the viscosity coefficient  $\beta$  and and c are the characteristics of the Powell Eyring model. Under usual boundary-layer and Boussinesq approximations, the governing boundary-layer equations of the continuity, momentum and energy for the steady flow can be written as:

$$\frac{\partial u}{\partial x} + \frac{\partial u}{\partial y} = 0 \tag{2}$$

$$u \frac{\partial u}{\partial x} + v \frac{\partial u}{\partial y} = \frac{1}{\rho_{\infty}} \frac{\partial}{\partial y} \left( \mu \frac{\partial u}{\partial y} + \frac{1}{\widetilde{\beta} c} \frac{\partial u}{\partial y} - \frac{1}{6\widetilde{\beta} c^3} \left( \frac{\partial u}{\partial y} \right)^3 \right)$$

$$- \frac{\mu}{\rho_{\infty} k} u - \frac{\sigma B^2}{\rho_{\infty}} u, \tag{3}$$

$$\rho_{\infty} c_p \left( u \frac{\partial T}{\partial x} + v \frac{\partial T}{\partial y} \right) = \frac{\partial}{\partial y} \left( \kappa \frac{\partial T}{\partial y} \right) + \frac{Q}{\rho_{\infty}} \left( T - T_{\infty} \right), \tag{4}$$

the boundary conditions are:

$$y = 0: u = u_w(x) + \frac{\lambda_1}{\mu_{\infty}} \left[ \frac{\partial u}{\partial y} + \frac{1}{\widetilde{\beta} c} \frac{\partial u}{\partial y} - \frac{1}{6\widetilde{\beta} c^3} \left( \frac{\partial u}{\partial y} \right)^3 \right],$$

$$v = 0, -\kappa \frac{\partial T}{\partial y} = h_f(T_f - T_w),$$

$$y \to \infty: \qquad u = 0, \qquad T \to T_{\infty}, \tag{5}$$

where T is the fluid temperature,  $T_{\infty}$  is the ambient temperature  $T_{\infty} < T_f$ ,  $\rho_{\infty}$  is the density of the fluid,  $\sigma$  is the electrical conductivity,  $c_p$  is the specific heat at constant pressure, k is the permeability of the porous medium, Q is the heat generation/absorption coefficient and  $\lambda_1$  is the slip parameter.

Now, we Introduce the non-dimensional quantities:

$$\eta = \sqrt{\frac{a}{v_{\infty}}}, u = axf'(\eta), v = -\sqrt{av_{\infty}}, \theta = \frac{T - T_{\infty}}{T - T_f}, (6)$$

the properties of the fluid (viscosity and thermal conductivity) is taken to be variable which defined as:

$$\mu = \mu_{\infty} e^{-\alpha \theta},\tag{7}$$

$$\kappa = \kappa_{\infty}(1 + \varepsilon\theta). \tag{8}$$

where  $v_{\infty}, \mu_{\infty}, \kappa_{\infty}$ , are the kinematic viscosity, dynamic viscosity, and the thermal conductivity of the fluid, $\alpha$  is the viscosity parameter and  $\kappa$  is the thermal conductivity parameter. From equations(2)-(8) we get the following system of ordinary differential equations:

$$f'''(e^{-\alpha\theta} + \gamma(1 - \beta f''^2)) + f''(f - \alpha e^{-\alpha\theta} \theta')$$
$$-f'^2 + f'(Ke^{-\alpha\theta} - M) = 0, \tag{9}$$
$$(1 + \varepsilon\theta)\theta'' + \varepsilon\theta'^2 + Pr(f\theta' + \gamma^*\theta) = 0, \tag{10}$$

with the boundary conditions

$$\begin{split} \eta &= 0: f' = 1 + \lambda (e^{-\alpha \theta} f'' + \gamma f'' - \frac{\gamma \beta}{3} f''^3), \\ f &= 0, (1 + \varepsilon \theta) \theta' = -\delta (1 - \theta), \\ \eta &\to \infty: \qquad f' = 0, \qquad \theta = 0, \end{split} \tag{11}$$

where,  $\gamma = \frac{1}{\mu_{\infty} \tilde{\beta} c}, \beta = \frac{a^3 x^2}{2c^2 V_{\infty}}$  are the dimensionless Powell-Eyring fluid parameters,  $K = \frac{v_{\infty}}{ak}$  is the porosity parameter,  $M = \frac{\sigma B^2}{a\rho_{\infty}}$  is the magnetic parameter,  $Pr = \frac{\mu_{\infty}c_p}{\kappa_{\infty}}$ is the Prandtl number,  $\lambda = \lambda_1 \sqrt{\frac{a}{v_{\infty}}}$  is the slip parameter,  $\gamma^* = rac{Q}{a
ho c_p}$  is the heat generation  $(\gamma^* > 0)$ /absorption  $(\gamma^* < 0)$  parameter and  $\delta = rac{h_f}{\kappa_{\!\scriptscriptstyle \infty}} \sqrt{rac{v_{\!\scriptscriptstyle \infty}}{a}}$  is the convective parameter. In fact, as  $\delta \to \infty$ , the boundary condition of  $\theta$ at the plate approaches the constant surface temperature (i.e. the boundary condition reduces to  $\theta(0) = 1$ ). We have important physical quantities are called the local



skin-friction coefficient  $Cf_x$  and the local Nusselt number  $Nu_x$  which defined as:

$$\frac{1}{2}Cf_xRe_x^{1/2} = -(e^{-\alpha\theta(0)} + \gamma)f''(0) + \frac{\gamma\beta}{3}f''(0)^3, \quad (12)$$

$$Nu_x Re_x^{-1/2} = -\theta'(0),$$
 (13)

where  $Re_x = \sqrt{\frac{xu_w}{V_\infty}}$  indicates the local Reynolds number.

# 3 Analytical Solutions

For the system of nonlinear differential equations (9) and (10) subject to boundary conditions(11), we can find the exact solutions  $f(\eta)$  and  $\theta(\eta)$  by taking  $\alpha = \gamma = \beta = \lambda = \varepsilon = 0$ . We Assume that

$$f(\eta) = \frac{1 - e^{-\omega \eta}}{\omega}, f''(0) = -\omega,$$

$$\omega = \sqrt{1 + M - K}, K < 1 + M. \tag{14}$$

Also, we can assume that

$$\xi(\eta) = \frac{-Pr}{\omega^2} e^{-\omega\eta} \tag{15}$$

then, equation (10) will transform to

$$\xi \theta'' + \theta' (1 - \xi - \frac{Pr}{\omega^2}) + \frac{Pr\gamma^*}{\omega \xi} \theta = 0, \tag{16}$$

subject to boundary conditions

$$\theta'(\xi = \frac{-Pr}{\omega^2}) = -\frac{\delta\omega}{Pr}(1 - \theta(\xi = \frac{-Pr}{\omega^2})), \quad \theta(0) = 0. \tag{17}$$

The exact solution of (16) with conditions (17)

$$\begin{split} \theta(\eta) = & (2\delta(e^{-\eta\omega})^{\frac{a+Pr}{2\omega^2}}\omega^3(U(\frac{a+Pr}{2\omega^2},1+\frac{a}{\omega^2}\\ &, -\frac{e^{-\eta\omega}Pr}{\omega^2})L_{-\frac{a+Pr}{2\omega^2}}^{\frac{\omega^2}{2\omega^2}}(0) - U(\frac{a+Pr}{2\omega^2},1+\frac{a}{\omega^2},0)\\ & L_{-\frac{a+Pr}{2\omega^2}}^{\frac{a}{2\omega^2}}(-\frac{e^{-\eta\omega}Pr}{\omega^2})))/(\omega^2(a+Pr+2\delta\omega)U(\frac{a+Pr}{2\omega^2}\\ &, 1+\frac{a}{\omega^2},-\frac{Pr}{\omega^2})L_{-\frac{a+Pr}{2\omega^2}}^{\frac{a}{2\omega^2}}(0) + (a\sqrt{Pr}+Pr)U(\\ & \frac{a+Pr+2\omega^2}{2\omega^2},2+\frac{a}{\omega^2},-\frac{Pr}{\omega^2})L_{-\frac{a+Pr}{2\omega^2}}^{\frac{a}{2\omega^2}}(0) - \omega^2U\\ & (\frac{a+Pr}{2\omega^2},1+\frac{a}{\omega^2},0)((a+Pr+2\delta\omega)L_{-\frac{a+Pr}{2\omega^2}}^{\frac{a}{2\omega^2}}\\ & (-\frac{Pr}{\omega^2})+2PrL_{-\frac{a+Pr+2\omega^2}{2\omega^2}}^{1+\frac{a}{2\omega^2}}(-\frac{Pr}{\omega^2}))), \end{split}$$

where  $a = \sqrt{Pr}\sqrt{Pr-4\omega^2\gamma^*}$ , U(a,b,c) is the confluent hypergeometric function and  $L_a^b(x)$  is the generalized Laguerre polynomial, the rate of heat transfer is given as:

$$\begin{split} \theta'(\eta) &= -(\delta(e^{-\eta\omega})^{\frac{a+Pr}{2\omega^2}+1}((a+Pr)(PrU(1+\frac{a+Pr}{2\omega^2}\\ ,2+\frac{a}{\omega^2},-\frac{e^{-\eta\omega}Pr}{\omega^2}) + e^{\eta\omega}\omega^2U(\frac{a+Pr}{2\omega^2},1+\frac{a}{\omega^2}\\ ,-\frac{e^{-\eta\omega}Pr}{\omega^2}))L_{-\frac{a^2}{2\omega^2}}^{\frac{a}{\omega^2}}(0) - \omega^2U(\frac{a+Pr}{2\omega^2},1+\frac{a}{\omega^2},0)\\ &(2PrL_{-1-\frac{a+Pr}{2\omega^2}}^{1+\frac{a}{\omega^2}}(-\frac{e^{-\eta\omega}Pr}{\omega^2}) + e^{\eta\omega}(a+Pr)L_{-\frac{a+Pr}{2\omega^2}}^{\frac{a}{\omega^2}}\\ &(-\frac{e^{-\eta\omega}Pr}{\omega^2}))))/(\omega^2(a+Pr+2\delta\omega)U(\frac{a+Pr}{2\omega^2},1\\ &+\frac{a}{\omega^2},-\frac{Pr}{\omega^2})L_{-\frac{a+Pr}{2\omega^2}}^{\frac{a^2}{\omega^2}}(0) + (a+\sqrt{Pr})\sqrt{Pr}U(\\ &\frac{a+Pr+2\omega^2}{2\omega^2},2+\frac{a}{\omega^2},-\frac{Pr}{\omega^2})L_{-\frac{a+Pr}{2\omega^2}}^{\frac{a^2}{\omega^2}}(0)\\ &-\omega^2U(\frac{a+Pr}{2\omega^2},1+\frac{a}{\omega^2},0)((a+Pr+2\delta\omega)\\ &L_{-\frac{a+Pr}{2\omega^2}}^{\frac{a}{\omega^2}}(-\frac{Pr}{\omega^2}) + 2PrL_{-\frac{a+Pr+2\omega^2}{2\omega^2}}^{1+\frac{a}{\omega^2}}(-\frac{Pr}{\omega^2}))), \end{split}$$

$$\theta'(0) = -(\delta((a+Pr)(PrU(1+\frac{a+Pr}{2\omega^2},2+\frac{a}{\omega^2},-\frac{Pr}{\omega^2})) + \omega^2 U(\frac{a+Pr}{2\omega^2},1+\frac{a}{\omega^2},-\frac{Pr}{\omega^2}))L_{-\frac{a+Pr}{2\omega^2}}^{\frac{a}{\omega^2}}(0) - \omega^2 U(\frac{a+Pr}{2\omega^2},1+\frac{a}{\omega^2},0)(2PrL_{-1-\frac{a+Pr}{2\omega^2}}^{1+\frac{a}{\omega^2}}(-\frac{Pr}{\omega^2})+(a+Pr)L_{-\frac{a+Pr}{2\omega^2}}^{\frac{a}{\omega^2}}(\frac{-Pr}{\omega^2}))))/(\omega^2(a+Pr+2\delta\omega)U(\frac{a+Pr}{2\omega^2},1+\frac{a}{\omega^2},-\frac{Pr}{\omega^2})L_{-\frac{a+Pr}{2\omega^2}}^{\frac{a}{\omega^2}}(0)+(a+\sqrt{Pr})$$

$$\sqrt{Pr}L_{-\frac{a+Pr}{2\omega^2}}^{\frac{a}{\omega^2}}(0)U(\frac{a+Pr+2\omega^2}{2\omega^2},2+\frac{a}{\omega^2},-\frac{Pr}{\omega^2})-\omega^2 U(\frac{a+Pr}{2\omega^2},1+\frac{a}{\omega^2},0)((a+Pr+2\delta\omega)L_{-\frac{a+Pr}{2\omega^2}}^{\frac{a}{\omega^2}}(-\frac{Pr}{\omega^2})+2Pr$$

$$L_{-\frac{a+Pr+2\omega^2}{2\omega^2}}^{1+\frac{a}{\omega^2}}(-\frac{Pr}{\omega^2}))).$$
(20)

In the next section, we will use equations (14) and (20) for testing the efficiency of the numerical method.

## 4 Numerical Results and Discussion

The numerical computations have been executed to the system of nonlinear differential equations (9) and (10) subject to boundary conditions(11) by fourth order



Runge-Kutta integration with the shooting scheme. In order to validate the method used in this study and to judge the accuracy of the present analysis, we have compared our results of the skin friction coefficient -f''(0) and the Nusselt number  $-\theta'(0)$  with the analytical solutions (14) and (20) as shown in Tables 1 and 2. The comparisons are found to be in good agreement.

Table 1: Comparison for the values of -f''(0) and  $-\theta'(0)$  with  $\alpha = \gamma = \beta = \lambda = \varepsilon = 0, \gamma^* = -0.3, \delta = 2, Pr = 0.72$ 

| M   | K   | -f'        | ''(0)     | $-\theta'(0)$ |           |  |  |
|-----|-----|------------|-----------|---------------|-----------|--|--|
|     |     | Analytical | Numerical | Analytical    | Numerical |  |  |
| 0.5 | 0.3 | 1.0954     | 1.0955    | .49839        | .49839    |  |  |
| 1.5 |     | 1.4832     | 1.4832    | .48020        | .48019    |  |  |
| 2   |     | 1.6432     | 1.6431    | .47399        | .47399    |  |  |
| 3   | 0.2 | 1.9494     | 1.9493    | .46382        | .46381    |  |  |
|     | 1   | 1.7321     | 1.7320    | .47083        | .47082    |  |  |
|     | 3   | 1.0000     | 1.0000    | .50365        | .50365    |  |  |

Table 2: Comparison for the values of  $-\theta'(0)$  with  $\alpha = \gamma = \beta = \lambda = \varepsilon = 0$ 

| M | K   | Pr   | δ   | $\gamma^*$ | $-\theta'(0)$ |           |  |
|---|-----|------|-----|------------|---------------|-----------|--|
|   |     |      |     |            | Analytical    | Numerical |  |
| 2 | 0.6 | 0.72 | 0.5 | -0.1       | 0.244106      | 0.244106  |  |
|   |     | 1    |     |            | 0.271116      | 0.271116  |  |
|   |     | 7    |     |            | 0.398376      | 0.398376  |  |
| 1 | 0.6 | 1.5  | 0.2 | 0.1        | 0.149696      | 0.149696  |  |
|   |     |      | 1   |            | 0.373105      | 0.373105  |  |
|   |     |      | 2   |            | 0.458671      | 0.458671  |  |
| 3 | 1   | 3    | 0.7 | -0.3       | 0.467468      | 0.467468  |  |
|   |     |      |     | 0.1        | 0.378481      | 0.378481  |  |
|   |     |      |     | 0.2        | 0.311204      | 0.311204  |  |

Undoubtedly, it is necessary for completing our study is clarifying effects of the introduced parameters on the velocity and temperature, figures 2-11 shows the influence of the parameters on the velocity f' and temperature  $\theta$ ,.

Figures 2 and 3 demonstrate the velocity and temperature distributions under the influence of two Powell-Eyring fluid parameters, we can notice that the velocity raises by  $\beta$  and  $\gamma$  increasing because the increment of these parameters increases the viscosity of fluid, while the temperature decreases with increasing

Figure 4 present the effectiveness of slip velocity parameter  $\lambda$  on the velocity and temperature profiles. It indicates that slip parameter reduces the velocity and enhances the temperature of the non-Newtonian fluid. The velocity and temperature profiles for different values of surface convection parameter  $\delta$  have been illustrated in Figure 5. It is clear that increasing  $\delta$  rises the temperature up, this is logical because the hot liquid at the surface heats it, and thus the heat is transferred to the fluid in successively. On contrary, the surface convection parameter  $\delta$  has a weak effect on decreasing velocity.

The variations of the dimensionless velocity and temperature against  $\eta$  for different values of the permeability parameter K are displayed in Figure 6. It is found that the velocity and temperature decreases with the increase in the permeability parameter because the increasing of porosity of the medium opposes the flow, which leads to enhanced deceleration of the flow. It is noticed from Figure 7 that the effect of Prandtl number is to reduce the dimensionless temperature, This is due to the fact that a fluid of larger Prandtl number retains a larger heat capacity; hence, a massive heat transfer.

Figure 8 depicts the variations of f' and  $\theta$  with the magnetic parameter M. It is observed that f' decreases with the increase in M along the surface. This is because that the application of a transverse magnetic field to an electrically conducting fluid excites a force of resistive-type called Lorentz force, which retards the motion of the fluid in the boundary layer. whilst, as the magnetic parameter M increase the temperature profiles decrease.

The graph for the velocity f' and temperature  $\theta$  is plotted for different values of the viscosity parameter  $\alpha$  in Figure 9, Which appears the weak effect of viscosity parameter on the velocity and temperature. It depict that the velocity decreases with increasing the values of  $\alpha$ , and the fluid viscosity increases the temperature of the fluid.

Figure 10 illustrates the effect of the heat source/sink parameter  $\gamma^*$  on the temperature distribution. Where  $\gamma^* > 0$  corresponds to internal heat generation and the case with  $\gamma^* < 0$  corresponds to internal heat absorption. It is clear from Fig. 10 that dimensionless temperature increases as increasing of heat generation because the energy is emitted at  $\gamma^* > 0$  and this causes the magnitude of temperature to increase, whereas the energy is realize at  $\gamma^* < 0$ , performing a noteworthy decrease in temperature near the boundary layer. Figure 11 displays the behavior of the velocity and temperature profiles under the influence of increasing thermal conductivity parameter. It is shown that increasing in thermal conductivity parameter raises the temperature of the fluid.

Computation through employed numerical scheme has been carried out for various non-dimensional values of dynamic parameters to studying the behavior of the local skin friction and the Nusselt number arising in the definitions (12) and (13) as shown in Table 3. We notice that, the local skin friction and the Nusselt number increases with increasing Prandtl number, this is because -as we mentioned earlier- a fluid with a higher value of Pr possesses a larger heat capacity so, the heat transfer was intensified. thus, cooling of the heated surface can be progressed by choosing a cooler has a larger Prandtl number.

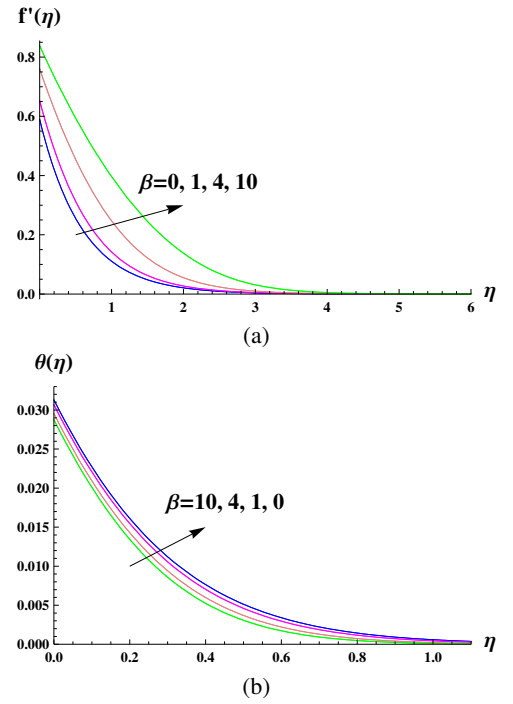


Figure 2:(a) Velocity and (b) temperature profiles for various values of  $\beta$  with  $Pr=10, \lambda=0.3, \delta=0.1, K=.3, \gamma=0.4, M=3, \alpha=0.5, \varepsilon=0.2, \gamma^*=-0.7$ 

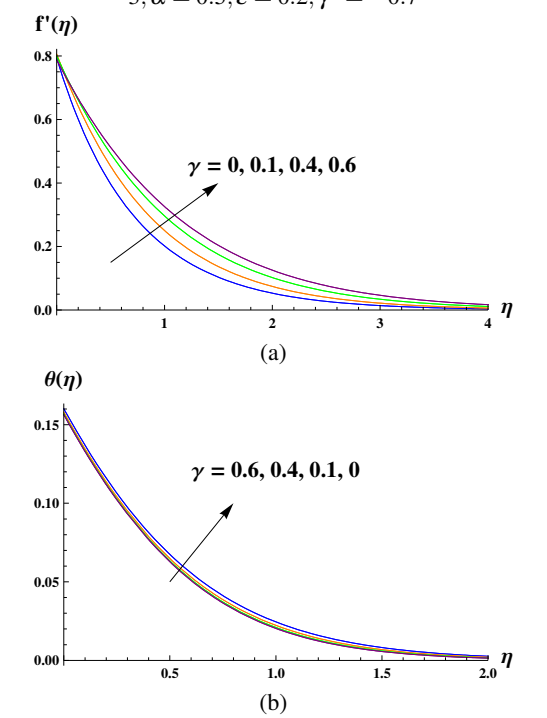


Figure 3: (a) Velocity and (b) temperature profiles for various values of  $\gamma$  with  $Pr=3, \lambda=0.2, \delta=0.3, K=.2, \beta=1, M=0.8, \alpha=0.5, \varepsilon=0.2, \gamma^*=-0.5$ 

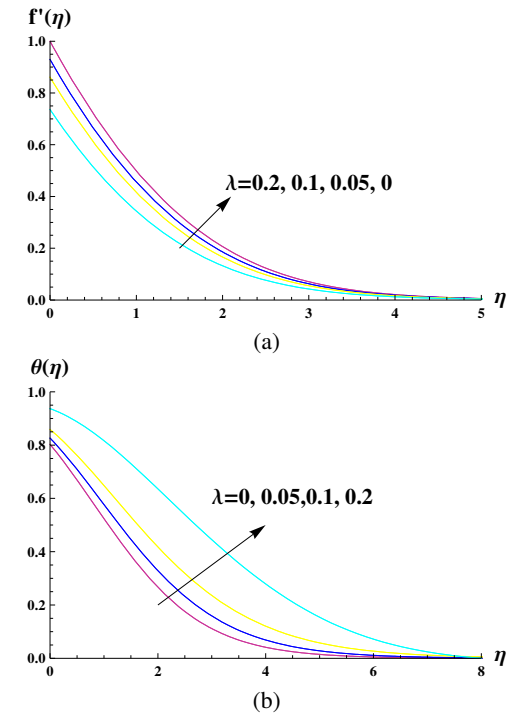


Figure 4:(a) Velocity and (b) temperature profiles for various values of  $\lambda$  with  $Pr=1, \gamma=3, \delta=2, K=.1, \beta=3, M=5, \alpha=1, \varepsilon=0.8, \gamma^*=0.2$ 

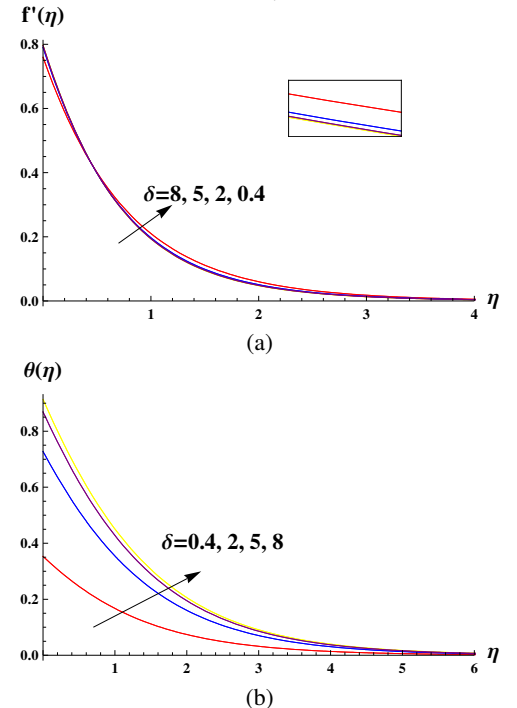


Figure 5:(a) Velocity and (b) temperature profiles for various values of  $\delta$  with  $Pr=0.72, \gamma=1, \lambda=0.2, K=0.2, \beta=0.3, M=1.8, <math>\alpha=3, \varepsilon=0.2, \gamma^*=-0.5$ 

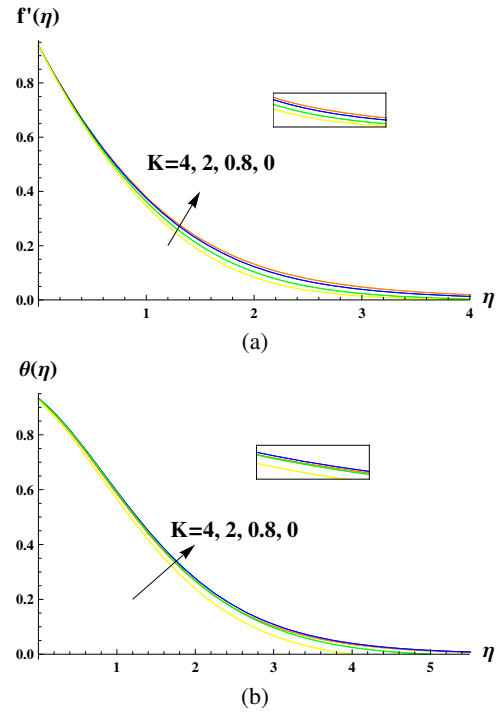


Figure 6: (a) Velocity and (b) temperature profiles for various values of K with  $Pr = 1.5, \gamma = 1, \lambda = 0.1, \delta = 4, \beta = 1, M =$  $0.5, \alpha = 5, \varepsilon = 0.2, \gamma^* = 0.3$ 

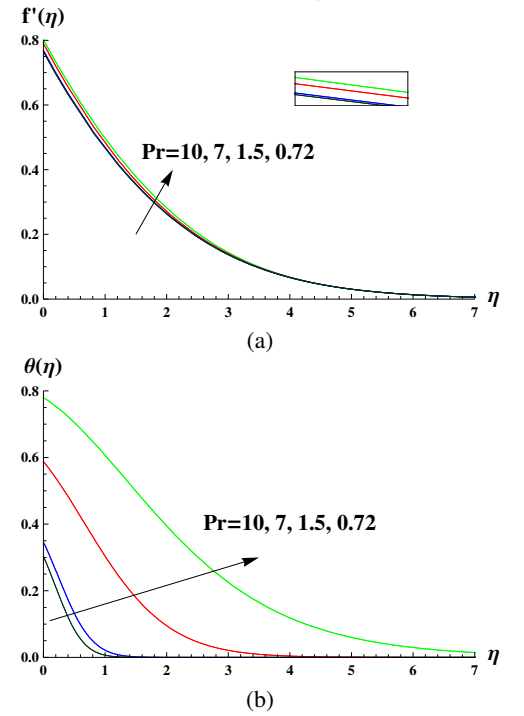


Figure 7:(a) Velocity and (b) temperature profiles for various values of *Pr* with  $K = 0.5, \gamma = 2, \lambda = 0.3, \delta = 0.6, \beta = 4, M =$  $0.5, \alpha = 2, \varepsilon = 0.2, \gamma^* = 0.3$ 

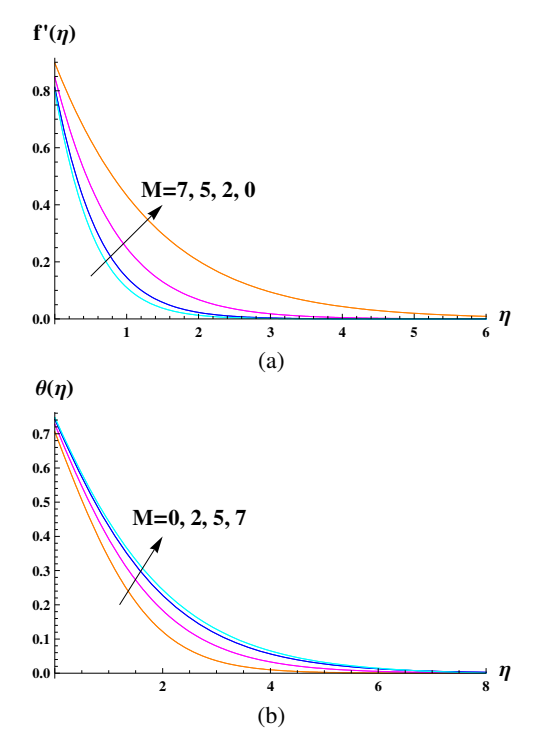


Figure 8:(a) Velocity and (b) temperature profiles for various values of *M* with  $K = 0.1, \gamma = 0.7, \lambda = 0.1, \delta = 2, \beta = 0.5, Pr =$  $1, \alpha = 0.05, \varepsilon = 0.6, \gamma^* = 0.7$ 

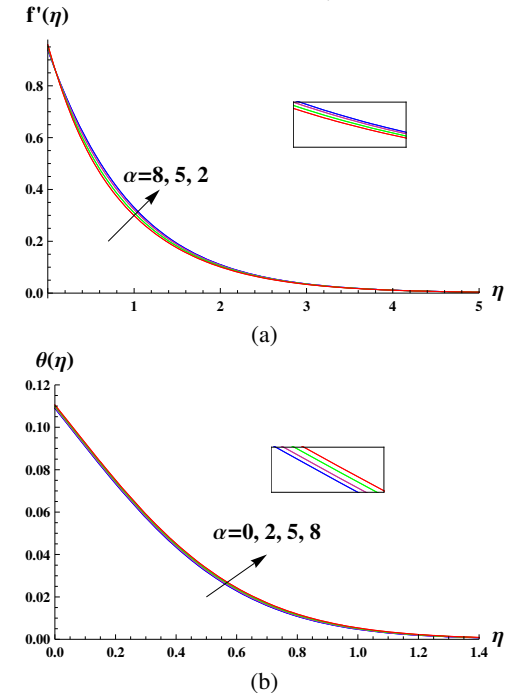


Figure 9:(a) Velocity and (b) temperature profiles for various values of  $\alpha$  with K = 0.3,  $\gamma = 0.4$ ,  $\lambda = 0.05$ ,  $\delta = 0.2$ ,  $\beta =$  $0.6, Pr = 7, M = 0.5, \varepsilon = 0.02, \gamma^* = 0.1$ 



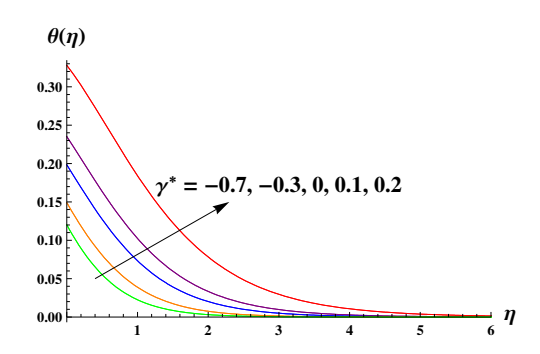


Figure 10:Temperature profiles for various values of  $\gamma^*$  with  $K=0.2, \gamma=0.3, \lambda=0.1, \delta=0.2, \beta=0.2, Pr=2, M=0.8, \varepsilon=0.5, \alpha=0.5$ 

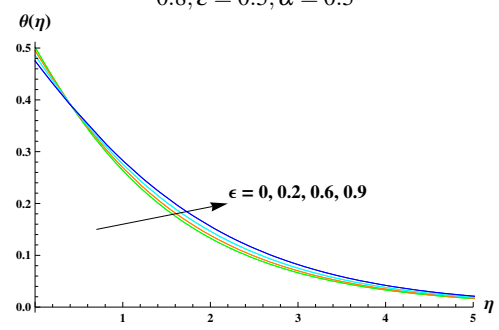


Figure 11:Temperature profiles for various values of  $\varepsilon$  with K = 0.5,  $\gamma = 0.2$ ,  $\lambda = 0.3$ ,  $\delta = 0.6$ ,  $\beta = 0.4$ , Pr = 0.72, M = 0.5,  $\gamma^* = 0.2$ ,  $\alpha = 2$ 

Also, it is observed that skin friction coefficient decreases with increasing  $\beta, \delta, \gamma$ , but the reverse is true for the local Nusselt number. It is also found that the local skin friction coefficient and the local Nusselt number decreases with increasing  $\alpha, \lambda$ . Moreover, it is found that the local skin friction increases and the local Nusselt number decreases with increasing  $K, M, \varepsilon$ .

Finally, it is noted that as the heat generation increase the local skin friction and the Nusselt number decrease. Because the heat generation will increase the fluid temperature near the plate and thus the heat transfer at the plate decrease and the temperature gradient at the surface decreases accordingly. While as the heat absorption increases the local skin friction and the local Nusselt number increases. This due to the fact that increasing the heat absorption creates to layer of cold fluid near to the heated surface.

#### Concluding Remarks

In this study, we concern to examine the effect of heat generation/absorption on a kind of MHD non-Newtonian fluid is called Powell-Eyring fluid having a variable viscosity and thermal conductivity exist in porous medium with slip velocity and convective condition at the surface. We formulate the system of partial differential equations with the boundary condition describing the

Table 3: Effect of the dynamic parameters on Local skin friction

| and Nusselt number |     |      |      |     |     |     |     |      |            |                                  |                    |
|--------------------|-----|------|------|-----|-----|-----|-----|------|------------|----------------------------------|--------------------|
| Pr                 | β   | α    | λ    | δ   | K   | М   | γ   | ε    | $\gamma^*$ | $-\frac{1}{2}Cf_{x}Re_{x}^{1/2}$ | $-Nu_xRe_x^{-1/2}$ |
| 0.72               | 4   | 2    | 0.3  | 0.6 | 0.5 | 0.5 | 2   | 0.2  | 0.3        | 0.6618                           | 0.1145             |
| 1.5                |     |      |      |     |     |     |     |      |            | 0.7015                           | 0.2215             |
| 7                  |     |      |      |     |     |     |     |      |            | 0.7706                           | 0.3677             |
| 10                 | 0   | 0.5  | 0.3  | 0.1 | 0.3 | 3   | 0.4 | 0.2  | -0.7       | 1.3700                           | 0.0963             |
|                    | 1   |      |      |     |     |     |     |      |            | 1.1607                           | 0.0963             |
|                    | 4   |      |      |     |     |     |     |      |            | 0.7984                           | 0.0965             |
| 7                  | 0.6 | 0    | 0.05 | 0.2 | 0.3 | 0.5 | 0.4 | 0.02 | 0.1        | 1.2427                           | 0.1778             |
|                    |     | 2    |      |     |     |     |     |      |            | 1.1319                           | 0.1778             |
|                    |     | 5    |      |     |     |     |     |      |            | 0.9735                           | 0.1776             |
| 1                  | 3   | 1    | 0    | 2   | 0.1 | 5   | 3   | 0.8  | 0.2        | 1.4229                           | 0.2406             |
|                    |     |      | 0.1  |     |     |     |     |      |            | 1.3889                           | 0.1678             |
|                    |     |      | 0.2  |     |     |     |     |      |            | 1.3193                           | 0.0723             |
| 0.72               | 0.3 | 3    | 0.2  | 0.1 | 0.2 | 1.8 | 1   | 0.2  | -0.5       | 2.8610                           | 0.0930             |
|                    |     |      |      | 2   |     |     |     |      |            | 1.0503                           | 0.4760             |
|                    |     |      |      | 5   |     |     |     |      |            | 1.0201                           | 0.5591             |
| 1.5                | 1   | 5    | 0.1  | 4   | 0   | 0.5 | 1   | 0.2  | 0.3        | 0.6193                           | 0.2340             |
|                    |     |      |      |     | 0.2 |     |     |      |            | 0.6199                           | 0.2267             |
|                    |     |      |      |     | 0.8 |     |     |      |            | 0.6215                           | 0.2070             |
| 1                  | 0.5 | 0.05 | 0.1  | 2   | 0.1 | 0   | 0.7 | 0.6  | -0.2       | 1.0307                           | 0.4136             |
|                    |     |      |      |     |     | 2   |     |      |            | 1.5243                           | 0.3792             |
|                    |     |      |      |     |     | 5   |     |      |            | 1.8807                           | 0.3565             |
| 7                  | 1   | 0.5  | 0.2  | 0.3 | 0.2 | 1.8 | 0   | 0.2  | 0.1        | 1.2113                           | 0.2308             |
|                    |     |      |      |     |     |     | 0.1 |      |            | 1.1307                           | 0.2343             |
|                    |     |      |      |     |     |     | 0.4 |      |            | 1.1143                           | 0.2378             |
| 0.72               | 0.4 | 2    | 0.3  | 0.6 | 0.5 | 0.5 | 0.2 | 0    | -0.3       | 0.6482                           | 0.2989             |
|                    |     |      |      |     |     |     |     | 0.2  |            | 0.6508                           | 0.2757             |
|                    |     |      |      |     |     |     |     | 0.9  |            | 0.6588                           | 0.2206             |
| 2                  | 0.2 | 0.3  | 0.1  | 0.2 | 0.2 | 0.8 | 0.3 | 0.4  | 0.2        | 1.2186                           | 0.1188             |
|                    |     |      |      |     |     |     |     |      | 0.1        | 1.2425                           | 0.1398             |
|                    |     |      |      |     |     |     |     |      | 0          | 1.2519                           | 0.1485             |
|                    |     |      |      |     |     |     |     |      | -0.3       | 1.2643                           | 0.1606             |
|                    |     |      |      |     |     |     |     |      | -0.7       | 1.2714                           | 0.167              |

problem, and using the symmetry transformation this system was transformed into a boundary value problem of ordinary differential equations.

Using shotting method, the system of ordinary differential is solved numerically, where it solved analytically at special case and we notice a great agreement between them. The influence of the parameters  $\beta, \gamma, \alpha, \lambda, \varepsilon, \gamma^*, Pr, K, M$  and  $\delta$  are examined graphically and their influence on local skin fraction and Nusselt number was tabulated numerically numerably.

We found an evident effect of the heat generation/absoption, convective parameter and the Prandtel number on the Nusselt number. Wherever, The local skin friction decreases by increasing the two parameters of the fluid, slip velocity parameter and the convective parameter and vice versa with respect to the permeability, magnetic and thermal conductivity parameters.

## References

- [1] P.S. Gupta, and A.S. Gupta, Heat and mass transfer on a stretching sheet with suction or blowing, *Can. J. Chem. Eng.*, 55, 744-746(1977).
- [2] E. Magyari and B. Keller, Heat and mass transfer in the boundary layers on an exponentially stretching continuous surface, *J. Phy. D: Appl. Phys*, 32, 577-585 (2000).
- [3] S. Mukhopadhyay, Unsteady boundary layer flow and heat transfer past a porous stretching sheet in presence of variable viscosity and thermal diffusivity, *Int. J. Heat Mass Trans.*, 52, 5213-5217 (2009).
- [4] A.M. Megahed, Variable viscosity and slip velocity effects on the flow and heat transfer of a power-law fluid over a



- non-linearly stretching surface with heat flux and thermal radiation. Rheol. Acta, 51,841-874(2012).
- [5] K. Sarada, R.J.P. Gowda ,I.E. Sarris, R.N. Kumar and B.C. Prasannakumara, Effect of Magnetohydrodynamics on Heat Transfer Behaviour of a Non-Newtonian Fluid Flow over a Stretching Sheet under Local Thermal Non-Equilibrium Condition, Fluids, 6(8), 264- (2021).
- [6] R.E. Powell and H. Eyring, Mechanism for relaxation theory of viscosity, Nature, 154, 427- 428(1944).
- [7] M. Patel and M.G. Timol, Numerical treatment of Powell-Eyring fluid flow using method of satisfaction of asymptotic boundary conditions, Appl. Num. Math, 59, 2584-2592(2009).
- [8] T. Hayat, Z. Iqbal, M. Qasim and S. Obaidat, Steady flow of an EyringPowell fluid over a moving surface with convective boundary conditions, Int. J. Heat Mass Trans., 55, 1817-1822(2012).
- [9] A. Mushtaq, M. Mustafa, T. Hayat, M. Rahi and A. Alsaedi, Exponentially stretching sheet in a Powell-Eyring fluid, Numerical and series solutions. Z. Naturforsch, 68a, 791-798(2013).
- [10] H. Zaman, Unsteady Incompressible Couette Flow Problem for the Eyring-Powell Model with Porous Walls, American J. Computational Math, 3, 313-325(2013).
- [11] A.M. Megahed, Flow and Heat Transfer of Powell-Eyring Fluid due to an Exponential Stretching Sheet with Heat Flux and Variable Thermal Conductivity, Zeitschrift für Natur forschung A, 70, 163-169 (2015).
- [12] M.A.A. Mahmoud and A.M. Megahed, Slip flow of Powell-Eyring liquid film due to an unsteady stretching sheet with heat generation, Brazilian Journal of Physics, 46 299-307(2016).
- [13] Khader, M. M. and Megahed, A. M., Numerical treatment for flow and heat transfer of Powell-Eyring fluid over an exponential stretching sheet with variable thermal conductivity, Meccanica, 51,1763-1770 (2016).
- [14] R. Khan, M. Zaydan, A. Wakif, B. Ahmed, R.L. Monaledi , I.L. Animasaun and A. Ahmed, A Note on the Similar and Non-Similar Solutions of Powell-Eyring Fluid Flow Model and Heat Transfer over a Horizontal Stretchable Surface, D.D.F., 401,2535 (2020).
- [15] D. Kumar, K. Ramesh, S. Chandok, Mathematical modeling and simulation for the flow of magneto-Powell-Eyring fluid in an annulus with concentric rotating cylinders, Chinese Journal of Physics, 65, 187-197(2020).
- [16] K. Vafai , Ambreen A. Khan , G. Fatima , Sadiq M. Sait , R. Ellahi, Dufour, Soret and radiation effects with magnetic dipole on Powell-Eyring fluid flow over a stretching sheet, International Journal of Numerical Methods for Heat Fluid Flow, 31(4), 1085-1103(2020).
- [17] M. Madhu, N.S. Shashikumar, B.J. Gireesha and N. Kishan, Thermal analysis of MHD PowellEyring fluid flow through a vertical microchannel, International Journal of Ambient Energy, (2021) DOI: 10.1080/01430750.2021.1910566.

Abeer S. Elfeshawey A lecturer in faculty of science, Banha University . Here research interests are in the areas of numerical solution for non-linear systems described some problems in fluid dynamics. She has published research articles in reputed international journals of mathematical and engineering sciences.

Shimaa E. Waheed Received the PhD degree in Applied Mathematics at Banha University . Here research interests are in the areas of applied mathematics and mathematical physics including numerical methods for non linear ordinary differential equations. She has published research articles in reputed international journals of mathematical and engineering sciences.